

# Electronic Structure of Molecules by (e,2e) Spectroscopy

JOHN H. MOORE\* and JOHN A. TOSSELL

*Chemistry Department, University of Maryland, College Park, Maryland 20742*

MICHAEL A. COPLAN

*Institute for Physical Sciences and Technology, University of Maryland, College Park, Maryland 20742*

*Received November 9, 1981 (Revised Manuscript Received March 31, 1982)*

The chemical and physical properties of atoms and molecules are directly related to the properties of their outer electrons. Measurements of dipole moment, polarizability, transition energy and probability, binding energy, and electron density are done routinely, to characterize electrons, and an important goal of theorists has been the calculation of the measured observables using *ab initio* wave functions. The application of coincidence techniques to the study of atomic and molecular systems now provides yet another method—(e,2e) spectroscopy.<sup>1</sup> The method is particularly sensitive to those aspects of electronic structure that are most important in determining the chemical and physical properties of atoms and molecules and as such provides an excellent test of *ab initio* calculations. In addition, the experiment provides symmetry information not readily available from other techniques. In this Account we describe the physical processes upon which (e,2e) spectroscopy is based and the theoretical interpretation of the results. Selected examples from recent studies are also presented.

The appellation (e,2e) is a term from the field of nuclear physics from which these experiments were derived. This designation refers to a knockout reaction in which a single incident electron knocks out a second target electron from the system of interest so that one starts with a single electron and finishes with two. From a chemist's point of view this is electron impact ionization. The binary (e,2e) process discussed here is high-energy, large momentum transfer electron impact ionization with complete determination of the electron kinematics and should be distinguished from the dipole (e,2e) experiment, which involves low momentum transfer by the incident electron to the knocked out electron. The dipole (e,2e) process is used to simulate

the photon in photoelectron spectroscopy.

The property observed in the binary (e,2e) experiment is the instantaneous value of the momentum of a single electron in an atom or molecule. While a chemist customarily describes a molecular electron in terms of its position relative to the nuclear framework, the connection between the momentum space and position space pictures is easily made. Consider a one-electron atom. The total electronic energy is the sum of the electron's potential and kinetic energies.

$$E = V + T$$

The energy  $E$  is constant and negative for a bound state. The potential energy  $V$  is negative while the kinetic energy  $T$  is, of course, always positive. As the electron approaches the nucleus, its potential energy falls and its kinetic energy, and therefore its momentum, increases in order to conserve the total energy. Thus large values of momentum are associated with small distances of the electron from the nucleus. Conversely, as the electron moves to large distances from the nucleus its potential energy increases at the expense of kinetic energy. Thus, large distances are associated with small values of momentum. It can be rigorously shown that the electron momentum distribution function or momentum density is equivalent to the electron spatial distribution function or electron density.

The (e,2e) experiment measures electron momentum by the conceptually simple scheme of knocking the electron out of an atom or molecule with another electron of known energy and momentum, and measuring simultaneously the energies and momenta of the knocked-out electron and scattered incident electron after the collision. By vector subtraction, the momentum of the knocked-out electron before the collision is then determined. By repeating the collision procedure over and over on a sample of identical atoms, one obtains a distribution of the possible momentum values of the electron—the momentum distribution function. Since the measured momenta used in the calculation of the knocked-out electron momentum are vector quantities, it is vital that their directions as well as magnitudes remain undistorted, before, during, and after the collision. To achieve this, the energy of the incident electron is made large compared to the binding energy of the target electron and only those collisions resulting in approximately equal energies and momenta for the knocked-out and scattered electron are considered.

Michael A. Coplan Received his Ph.D. from Yale University in 1963. He subsequently spent 2 years at the University of Paris conducting research in electrochemistry and 2 years at the University of Chicago studying chemical kinetics in shock waves. He joined the faculty of the University of Maryland in 1967, where he currently holds the position of Research Professor in the Institute of Physical Sciences and Technology. In addition to his work in electron spectroscopy, he is carrying out studies of the solar wind with an instrument aboard the ISEE-3 spacecraft.

John A. Tossell received a Ph.D. in physical chemistry from Harvard University in 1972 and did postdoctoral work in mineralogy with Professor R. G. Burns at MIT for 2 years. In 1973 he joined the faculty at the University of Maryland where he is now an Associate Professor. His current research focuses on quantum mechanical studies of inorganic compounds and minerals.

John H. Moore received his Ph.D. in physical chemistry from The Johns Hopkins University in 1967. He spent 2 additional years at Johns Hopkins developing the technique of ion impact spectroscopy and then joined the faculty of the University of Maryland in 1969, where he is Professor of Chemistry. He has been a JILA Visiting Fellow and a Program Officer with the National Science Foundation. His research work includes electron transmission spectroscopy and instrument development for space exploration.

(1) McCarthy, I. E.; Weigold, E. *Phys. Rep.* 1976, 27, 275.

In addition, the binding energy of the atomic electron is determined from the scalar difference between the kinetic energy of the incident electron and the sum of the knocked-out and scattered electron kinetic energies. The measured binding energy can be compared with that obtained by photoelectron spectroscopy with the sole difference being that the (e,2e) measurement is made over a large range of target electron momenta, while the photoelectron measurement is at a fixed value of target electron momentum, which depends on the incident photon energy,  $h\nu$ , and electron binding energy. This follows from the conservation of momentum since all of the photon's momentum ( $h\nu/c$ ) is transferred to the target electron.

The electron momentum distribution that is measured in the (e,2e) experiment is particularly useful in the interpretation of many chemical phenomena. This follows from the properties of the momentum space wave function from which the momentum density is derived. The single electron momentum distribution function  $\rho(\vec{q})$  is simply the square modulus of the momentum space wave function  $\chi(\vec{q})$  (where  $\vec{q}$  is the symbol for momentum) just as the single electron density  $\rho(\vec{r})$  is the square of the spatial wave function  $\phi(\vec{r})$ . The momentum space function and the position space function are uniquely related by an integral transformation, the Fourier transform.  $\chi(\vec{q})$  tends to have its greatest amplitude at small values of  $\vec{q}$  corresponding to large values of  $\vec{r}$ . That is,  $\chi(\vec{q})$  and  $\phi(\vec{r})$  emphasize inverse regions of their respective spaces.<sup>2</sup> Thus  $\chi(\vec{q})$  is most sensitive to the diffuse portions of the spatial wave function—the tail of the wave function at large distances from the nuclear framework. It is this tail of the wave function and the corresponding electron density that accounts for through-space interactions, conjugation, and the weak molecular association that leads to chemical reaction.

When attempting to understand such phenomena, a chemist often relies upon Hückel approximate wave functions or similar minimum basis set models. However, because the amplitude of a position space wave function is very small at large distances, it is difficult to discern the discrepancy between a very simple model and the electron density predicted by a more sophisticated wave function or the electron density that actually exists in nature. This problem in assessing the quality of a model is overcome if one adopts the momentum space representation. Furthermore, by simply taking the square modulus of an approximate single-electron wave function in momentum space to obtain the momentum distribution function, a comparison can be made with the momentum density obtained from the (e,2e) experiment. No such opportunity is practical for comparison between a model and experiment in the position space representation.

A chemist often relies upon symmetry arguments to gain an understanding of chemical phenomena. The power of these arguments carries over to the momentum space view of electronic behavior afforded by (e,2e) spectroscopy since all of the symmetry properties of a molecular wave function are preserved. Because the position space wave function and momentum space wave function are only different representations of the

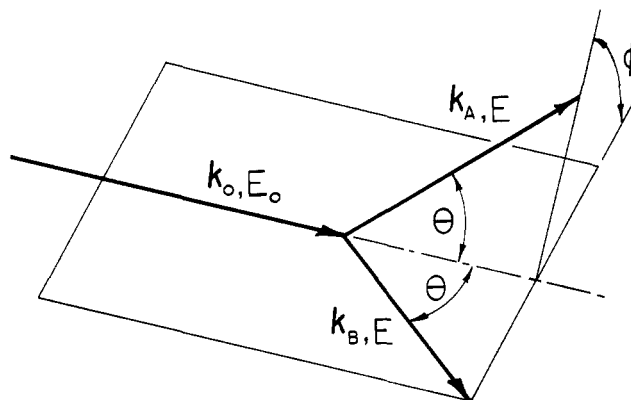


Figure 1. The symmetric noncoplanar geometry for the (e,2e) experiment.

same vector in Hilbert space, they possess the same eigenvalues for all operators and, in particular, for the symmetry operators of the molecular point group. The momentum space wave function and the corresponding position space wave function therefore belong to the same irreducible representation. The value of a function at the origin in either space may be nonzero if and only if it transforms as the totally symmetric irreducible representation. The momentum wave function and the corresponding momentum density for an electron in an orbital that is not totally symmetric must have a node at zero momentum. Thus, an atomic s orbital and a p orbital have distinctively different momentum functions. For the s orbital,  $\rho(\vec{q})$  is a maximum at  $q = 0$  while for the p orbital  $\rho(\vec{q})$  is zero at  $q = 0$  and increases to a maximum at an intermediate value of  $q$ . A similar difference distinguishes the  $\sigma_g$  orbital of a homonuclear diatomic molecule from other orbitals. Similarly, an  $a_g$  orbital of a polyatomic molecule is distinguished from, say, a  $b_{3u}$ , as will be illustrated below.

This qualitative difference of the momentum space functions can provide valuable information for the chemist. For example, the shape of the momentum distribution is quite sensitive to the change of symmetry which accompanies molecular distortion. Similarly, orbital mixing or hybridization is reflected in the momentum distribution. Thus (e,2e) spectroscopy, by providing both energy and symmetry information, is superior to conventional spectroscopies. For example, the assignment of peaks in a photoelectron spectrum is basically an intuitive process. With the addition of symmetry information from (e,2e) spectroscopy, ionization potentials can often be assigned unambiguously.

## The Experiment

The (e,2e) process is most easily interpreted in terms of momentum densities when the experiment is done in the symmetric, noncoplanar geometry illustrated by the vector diagram in Figure 1. The kinetic energy,  $E_A$  and  $E_B$ , available to the outgoing electrons is the incident energy,  $E_o$ , minus the binding energy, BE, of the target electron. This is equally divided between the outgoing electrons so that

$$E_A = E_B = (E_o - BE)/2$$

Both outgoing electrons exit at the same polar angle,  $\theta$ , with respect to the incident direction. This angle is fixed at  $45^\circ$  to best satisfy the approximations used in interpreting the experiment and to permit measurement

(2) Epstein, I. R.; Tanner, A. C. In "Compton Scattering"; Williams, B., Ed.; McGraw-Hill: New York, 1977; Chapter 7.

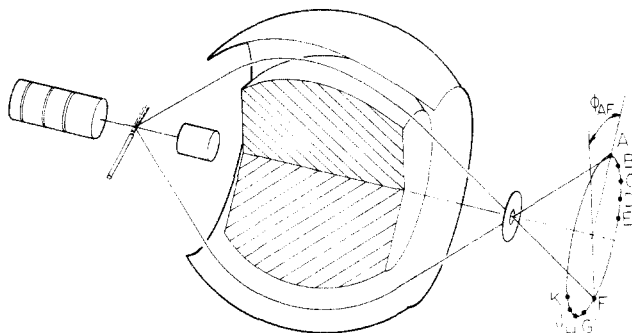


**Figure 2.** The (e,2e) apparatus. An electrical potential placed across the spherical electrodes deflects electrons of a particular kinetic energy through a common energy-resolving aperture. An electron pair whose planes of deflection are oriented at an azimuthal angle of, say,  $\phi_{AF}$  with respect to one another are detected in coincidence by detectors at points A and F.

of the momentum density over the largest possible range. The independent variable is the azimuthal angle,  $\phi$ , between the momentum vector  $\vec{k}_B$  and the plane defined by  $\vec{k}_0$  and  $\vec{k}_A$ . The magnitude of the momentum of the target electron,  $q$ , at the instant of collision is a simple monotonic function of the azimuthal angle and is given by

$$q = |\vec{q}| = \left[ (2|\vec{k}_A| \cos \theta - |\vec{k}_0|)^2 + (2|\vec{k}_A| \sin \theta \sin \phi/2)^2 \right]^{1/2}$$

Since the determination of  $q$  depends on the simultaneous measurement of  $\vec{k}_A$  and  $\vec{k}_B$  in the presence of electrons from all other collision processes, timing resolution of the order of  $10^{-9}$  s is required to distinguish the electrons of interest from the others.

The first (e,2e) experiment used two separate energy analyzer/detector units each positioned to intercept one of the pair of electrons leaving the scattering center at a particular azimuthal angle with respect to one another.<sup>3</sup> The coincidence count rate then gave the probability of the target electron's possessing the corresponding value of  $q$ . After a collection time of the order of an hour, one unit was moved relative to the other, and another point on the distribution curve was determined.

We have developed a multichannel device<sup>4</sup> that enables us to sample many points on the momentum density curve at the same time. The instrument is based upon a doubly truncated, spherical, electrostatic electron energy analyzer illustrated in Figure 2. Electrons of the appropriate energy and polar angle are transmitted independent of their azimuthal angle. Electrons exit along the surface of a coaxial cone where they are intercepted by an annular array of detectors positioned so that every pair corresponds to a different azimuthal angle. The coincidence rate is monitored at 25 azimuthal angles simultaneously, and thus the entire momentum distribution is measured at once.

### Theoretical Interpretation

To establish the connection between the (e,2e) process and the momentum density it is most convenient

to use the plane wave impulse approximation.<sup>5</sup> Of course, the experiment must be carried out in a manner that justifies this approximation. The triply differential (e,2e) cross section for the knock-out of an electron from the  $j$ th orbital of a molecule with total wave function  $\Psi$  to produce an ion with a total wave function  $\Phi$  is given by

$$\frac{d^3\sigma}{dE d\Omega_1 d\Omega_2} = \sigma_{(e,2e)} = \frac{4|\vec{k}_A||\vec{k}_B|}{|\vec{k}_0|} \sigma_{(e,e)} |\langle \Phi | e^{i(\vec{k}_0 - \vec{k}_A - \vec{k}_B) \cdot \vec{r}} | \Psi \rangle|^2$$

where  $\sigma_{(e,e)}$  is the electron-electron cross section in the center of mass of the two electrons. If  $\Psi$  and  $\Phi$  are both independent orbital single configuration product wave functions, the cross section reduces to

$$\sigma_{(e,2e)} = \frac{4|\vec{k}_A||\vec{k}_B|}{|\vec{k}_0|} \sigma_{(e,e)} |\langle \Phi | \Phi_j \rangle|^2 |\langle e^{i\vec{q} \cdot \vec{r}} | \phi(\vec{r}_j) \rangle|^2$$

where  $\Phi_j$  is now the wave function for the target minus the unoccupied  $j$ th orbital and  $\phi(\vec{r}_j)$  is the single  $j$ th orbital wave function. The first squared term is called the spectroscopic factor and is approximately equal to unity when the passive orbitals of the target and residual ion are nearly the same. The last term, the square of the Fourier transform of the single electron orbital  $\phi(r_j)$ , is the square of the wave function for the  $j$ th orbital in momentum space  $|\chi_j(\vec{q})|^2$ . This term is the single electron momentum density  $\rho_j(q)$ .

It is often the case that the removal of a single electron from a molecule with filled orbitals results in the excitation of a second electron because of correlation effects.<sup>6,7</sup> This is the origin of the satellite structure often seen in photoelectron spectra. The existence of such satellites requires that a configuration interaction (CI) wave function be used rather than the single configuration wave function which is adequate for simple systems. The most rudimentary CI ion wave function consists of a single hole function  $C_k \Phi_k$  plus a sum of single excitation functions  $\sum_{j\alpha} C_{kj\alpha} \Phi_{kj\alpha}$  where the subscript  $kj\alpha$  indicates a hole in orbital  $k$  and excitation from orbital  $j$  to unoccupied orbital  $\alpha$ . These excited configurations must obviously have the same symmetry as the primary configuration. By substituting this CI wave function for  $\Phi$  in the expression for  $\sigma_{(e,2e)}$  and assuming that different single orbitals of the target and ion are orthogonal, it can be shown that the amplitude of the satellite is proportional to  $|C_k|^2$  and the shape of the momentum density is identical with that of the primary hole. If the orbitals of the target molecule and ion differ significantly due to relaxation effects, the momentum densities of the primary and satellite peaks will differ somewhat.

In the following section, examples showing the usefulness of the (e,2e) technique for testing the quality of theoretical wave functions and assigning satellite structure will be given and the effect of nuclear motion on electronic structure demonstrated. Finally, the autocorrelation function  $B(r)$  will be introduced and its usefulness in interpreting (e,2e) data discussed.

(3) Amaldi, U.; Egidi, A.; Marconero, R.; Pizzella, G. *Rev. Sci. Instrum.*, **1969**, *40*, 1001. Camilloni, R. Giardini-Guidoni, A.; Tiribelli, R.; Stefani, G. *Phys. Rev. Lett.* **1972**, *29*, 618.

(4) Moore, J. H.; Coplan, M. A.; Skillman, T. L.; Brooks, E. D. *Rev. Sci. Instrum.* **1978**, *49*, 463. Skillman, T. L.; Brooks, E. D.; Coplan, M. A.; Moore, J. H. *Nucl. Instrum. Methods* **1978**, *159*, 267.

(5) Neudatchin, V. G.; Novoskol'tseva, G. A.; Smirnov, Yu. F. *Sov. Phys. JETP (Engl. Transl.)* **1969**, *28*, 540; Glassgold, A. E.; Ialongo, G. *Phys. Rev.* **1968**, *175*, 151.

(6) Levin, V. G. *Phys. Lett.* **1972**, *394*, 125.

(7) Coplan, M. A.; Migdall, A. L.; Moore, J. H.; Tossell, J. A. *J. Am. Chem. Soc.* **1978**, *100*, 5008.

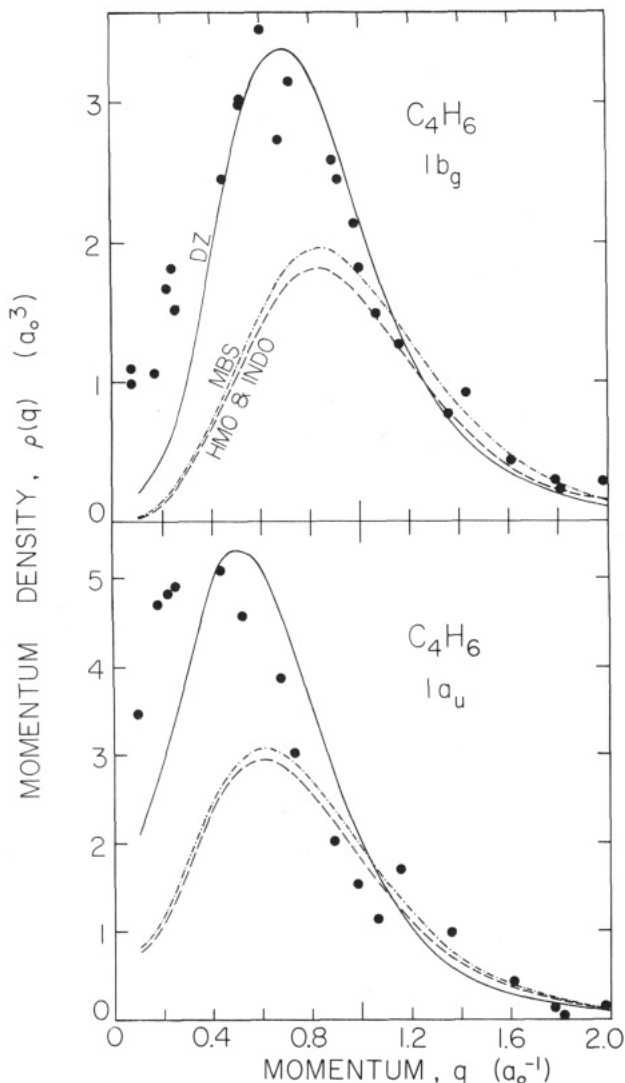


**Figure 3.** Momentum densities measured for the  $\pi$  orbitals of butadiene. Momentum densities predicted by INDO approximate SCF, Hückel molecular orbital (HMO), minimum basis set (MBS), and double- $\zeta$  (DZ) Gaussian orbital SCF wave functions are shown for comparison.

### Comparison of Theoretical Momentum Densities with Experiment

Momentum densities for the  $\pi$  orbitals of butadiene<sup>8</sup> are displayed in Figure 3. In addition to the experimental results, momentum densities predicted from minimum basis set (MBS) wave functions,<sup>9</sup> Hückel (HMO) wave functions, INDO approximate SCF wave functions,<sup>10</sup> and double- $\zeta$  (DZ) Gaussian orbital SCF wave functions<sup>11</sup> are given. Both  $a_u$  and  $b_g$  spherically averaged momentum densities have the characteristic p orbital shape. They differ in that the all-bonding  $1a_u$  momentum density has a maximum at a lower value of momentum than does that of the  $1b_g$  orbital, which is antibonding between C-2 and C-3. This difference can be understood in terms of position space differences

(8) Coplan, M. A.; Moore, J. H.; Tossell, J. A.; Gupta, A. *J. Chem. Phys.* 1979, 71, 4005.

(9) Switkes, E.; Stevens, R. M.; Lipscomb, W. N. *J. Chem. Phys.* 1969, 51, 5229.

(10) Pople, J. A.; Beveridge, D. L., "Approximate Molecular Orbital Theory"; McGraw-Hill: New York, 1970.

(11) Snyder, L. C.; Basch, H., "Molecular Wave Functions and Properties"; Wiley: New York, 1972.

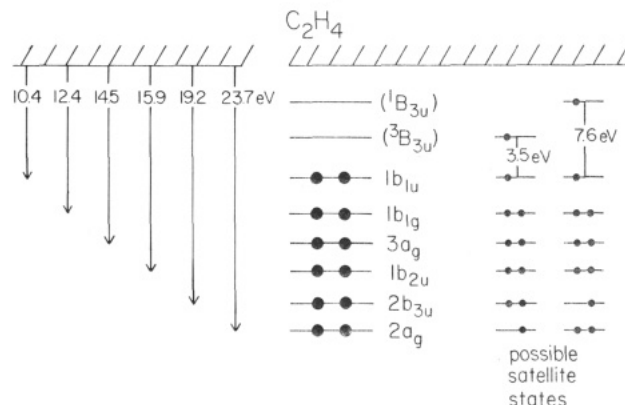


**Figure 4.** Binding energies of the valence electrons of ethylene and possible satellite states arising from simultaneous ionization and excitation.

between the two wave functions. The  $1a_u$  is more diffusely distributed than the  $1b_g$ . Because of the Fourier transform relation between position and momentum space, the more diffuse orbital has a greater momentum density at low momentum. Recall also that the average value of the momentum is obtained as the expectation value of the gradient operator  $\nabla$  in position space. The rapid variation of the  $1b_g$  function as it passes through the node between C-2 and C-3 tends to increase the amplitude of the momentum space wave function at high values of momentum. These considerations also account for the difference between the theoretical wave functions. In comparison to the double- $\zeta$  functions the MBS, INDO, and HMO functions do not adequately represent the diffuse parts of the electron density. In addition, the more limited functions vary too rapidly in passing through the node of the  $1b_g$  orbital. The superiority of the double- $\zeta$  wave function in momentum space does not adequately account for the momentum density at low momentum.

### The Assignment of Satellite Structure

In the photoelectron spectrum of ethylene in the valence region a satellite peak appears at 27.4 eV in addition to the six primary peaks expected for electron ejection from each of the six valence orbitals.<sup>12</sup> The origin of the satellite had been an open question since, as illustrated in Figure 4, there are two energetically equivalent possibilities: configuration interaction in the  ${}^2B_{3u}$  ion state arising from removal of an electron from the  $2b_{3u}$  orbital or configuration interaction in the  ${}^2A_g$  state associated with a  $2a_g$  hole. The (e,2e) cross section as a function of the knocked-out electron energy over the region corresponding to the four innermost valence orbitals and the satellite is shown in Figure 5. Except for the rather lower energy resolution, this spectrum is similar to a photoionization spectrum. The reduced intensity of the  $2a_g$  primary peak immediately suggests that the  $2a_g$  hole state is the parent of the satellite. Measurement of the momentum densities of the satellite and the  $2b_{3u}$  and  $2a_g$  primary peaks has conclusively established this to be the case.<sup>7</sup> As shown in Figure 6, the  $2b_{3u}$  orbital momentum density has the characteristic p orbital shape, while the  $2a_g$  has the

(12) Banna, M. S.; Shirley, D. A. *J. Electron Spectrosc. Relat. Phenom.* 1976, 8, 255.

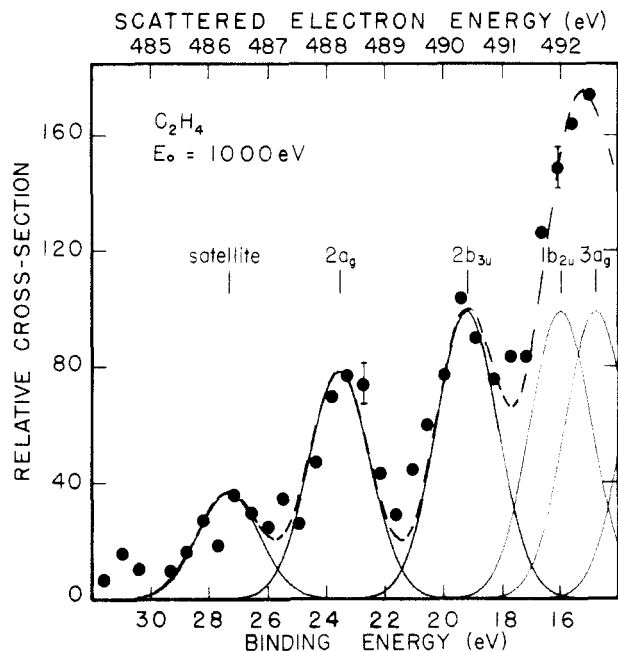


**Figure 5.** (e,2e) cross section as a function of binding energy for the four innermost valence orbitals and the 27.4-eV satellite of ethylene.

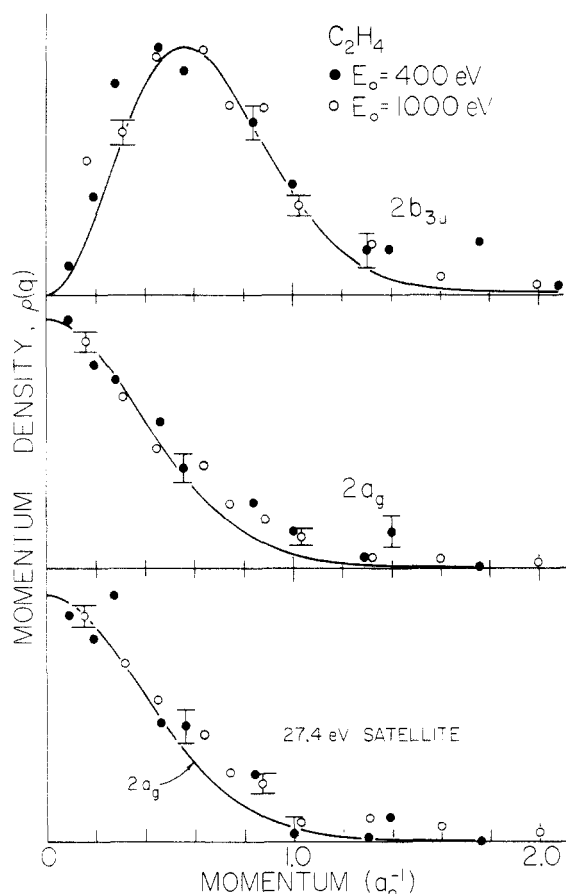


**Figure 6.** Measured momentum densities for the two innermost valence orbitals and the 27.4 eV satellite of ethylene. The  $2a_g$  orbital is clearly the parent of the satellite.

shape characteristic of a totally symmetric orbital. The momentum density for the satellite is identical in shape to that of the  $2a_g$ . Furthermore, a comparison of the magnitude of the (e,2e) cross section of the satellite to that for the  $2a_g$  gives a ratio of  $0.47 \pm 0.07$ , and a CI wave function calculated by Martin and Davidson<sup>13</sup>

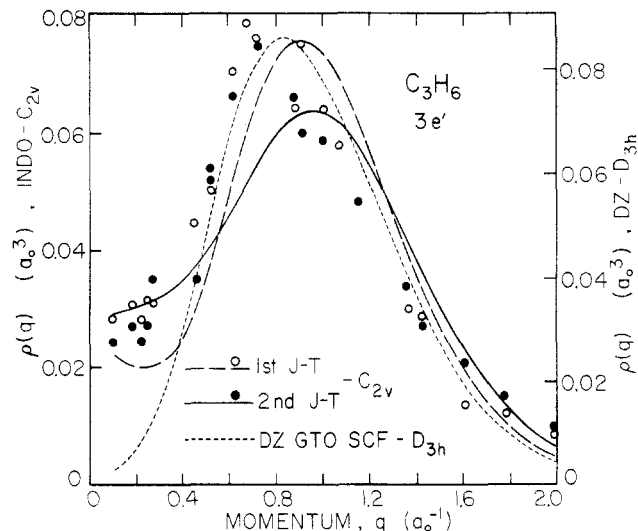


**Figure 7.** Measured momentum density for each of the Jahn-Teller components corresponding to the  $3e'$  orbital of cyclopropane. Momentum densities given by INDO wave functions for the  $C_{2v}$  geometry and a double- $\zeta$  wave function for the  $D_{3h}$  geometry are shown for comparison.

gives the square of the ratio of the corresponding CI coefficients,  $(C_{2a_g}^{\text{satellite}}/C_{2a_g}^{\text{primary}})^2 = 0.30$ , in reasonable agreement with our observation given the limited basis set used in the calculation.

### The Effect of Nuclear Motion on the Momentum Density

The momentum density for electrons in the  $3e'$  orbital of cyclopropane is displayed in Figure 7. It is obvious that the momentum density does not go to zero at  $q = 0$  in spite of the fact that symmetry considerations require that the momentum wave function of a doubly degenerate orbital have a node at  $q = 0$ . The cause of this discrepancy is the doubly degenerate  $e'$  vibration of the cyclopropane molecule.<sup>14</sup>

To understand the connection between this vibrational mode and the observed momentum density one must realize that when a doubly degenerate mode exists the most probable geometry is different from the equilibrium geometry.<sup>15</sup> Thus, on the average the molecule is distorted into a geometry of  $C_{2v}$  symmetry from the equilibrium  $D_{3h}$  symmetry. This distortion splits the  $3e'$  molecular orbital into two orbitals corresponding to the respective Jahn-Teller components,<sup>16</sup> each of which is a mixture of orbitals of  $a_1$  and  $b_2$  functions in  $C_{2v}$  symmetry. The admixture of the totally symmetric  $a_1$  term arising from the molecular distortion accounts for the observed amplitude at zero momentum in the momentum density. To illustrate this, momentum densities based upon simple INDO wave functions<sup>10</sup> for two orthogonal distorted geometries of cyclopropane have been calculated. For comparison, the momentum density predicted by a double- $\zeta$  wave function<sup>11</sup> for the undistorted molecule is also shown. The fact that the (e,2e) technique is sensitive to this interaction of nuclear and electronic motion is

(13) Martin, R. L.; Davidson, E. R. *Chem. Phys. Lett.* **1977**, *51*, 237.

(14) Tossell, J. A.; Moore, J. H.; Coplan, M. A. *Chem. Phys. Lett.* **1979**, *67*, 356.

(15) Sturge, M. D. *Solid State Phys.* **1967**, *20*, 91 (see, in particular, p 188).

(16) Basch, H.; Robin, M. B.; Kuebler, N. A.; Baker, C.; Turner, D. W. *J. Chem. Phys.* **1969**, *51*, 52.

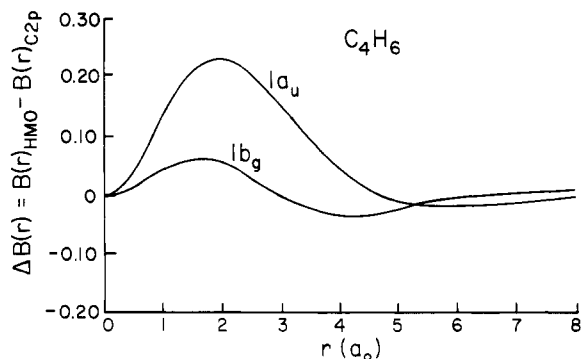


**Figure 8.** The differences between the autocorrelation function  $B(r)$  calculated from Hückel molecular orbital wave functions for the  $\pi$  orbitals of butadiene and  $B(r)$  calculated for a single Slater  $2p$  orbital of the same exponent.

a further demonstration of its usefulness.<sup>17</sup>

### The Autocorrelation Function and Chemical Bonding

While direct comparison between experimentally measured momentum densities and theoretical calculations are useful for elucidating electronic structure, it would be even more useful if there were a function, derivable from experimental momentum densities, which emphasized the sensitivity of the experiment to the chemically important regions of the spatial wave function and at the same time could be interpreted in terms of familiar chemical bonding models. Such a function exists and is called  $B(\vec{r})$ ; it is the Fourier transform of the momentum density and is equivalent to the autocorrelation function of the spatial wave function<sup>18</sup>

$$B_k(\vec{r}) = \int \rho_k(\vec{q}) e^{-i\vec{q}\cdot\vec{r}} d\vec{q} = \int \phi_k(\vec{s}) \phi_k(\vec{s} + \vec{r}) d\vec{s}$$

$B(\vec{r})$  is large when  $\phi_k$  has large amplitude at points separated by  $\vec{r}$ . This function is analogous to the structure factor in X-ray diffraction, which is the Fourier transform of the electron density. Only the spherically averaged momentum density can be obtained from the (e,2e) experiment on molecules in the gas phase. Fortunately, however, it can be shown that the Fourier transform of a spherically averaged single-electron momentum density yields the spherical average of the corresponding  $B(\vec{r})$  function,<sup>19</sup> which is still quite rich in chemical information, particularly when the differences  $\Delta B(r)$  between  $B(r)$  functions for different theoretical wave functions, or between experimental and theoretical  $B(r)$  functions for the same orbital are taken. As an example, we show in Figure 8, for the  $1a_u$  and  $1b_g$  orbitals of butadiene, the HMO  $B(r)$  functions minus  $B(r)$  calculated for a single Slater  $2p$  orbital of the same orbital exponent as that used in the MO. This  $\Delta B(r)$  emphasizes the effect of chemical bonding upon the autocorrelation function. The most significant feature occurs near  $r = 2a_0$ , which implies that the molecular wave functions have a large amplitude of the same sign

(17) Levin, V. G.; Neudatchin, V. G.; Pavitchenkov, A. V.; Smirnov, Yu. F. *J. Chem. Phys.* 1975, 63, 1541.

(18) Benesch, R.; Singh, S. R.; Smith, V. H. *Chem. Phys. Lett.* 1971, 10, 151. Schulke, W. *Phys. Status Solidi B* 1977, 82, 229. Weyrich, W.; Pattison, P.; Williams, B. G. *Chem. Phys.* 1979, 41, 271.

(19) Tossell, J. A.; Moore, J. H.; Coplan, M. A. *J. Electron Spectrosc. Relat. Phenom.* 1981, 22, 61.

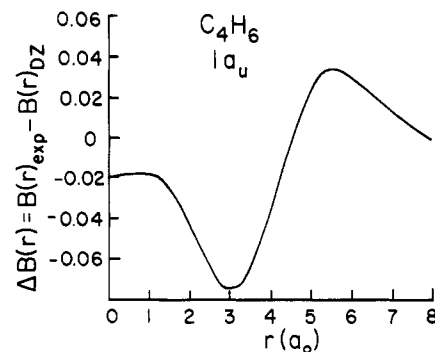


**Figure 9.** The difference between  $B(r)$  obtained from the (e,2e) experiment and  $B(r)$  calculated from the double- $\zeta$  wave function.

at locations separated by this value of  $r$ . This feature in  $\Delta B(r)$  for the  $1a_u$  is larger than for the  $1b_g$  since the net number of C-C  $\pi$ -bonding interactions for the former is three and for the latter only one.

A similar analysis can be employed in comparing experimental and theoretical results. In Figure 9 we show for the  $1a_u$  orbital of butadiene the difference between the  $B(r)$  function obtained from the (e,2e) experiment and that calculated from the double- $\zeta$  approximate molecular wave function. The chief features are a negative region between  $2a_0$  and  $4a_0$  and a positive region beyond  $5a_0$ . Qualitatively speaking, this implies that the probability of two electrons being separated by  $2a_0$ – $4a_0$  is less than predicted by the approximate wave function, while the probability of their being separated by  $5a_0$  is greater in fact than is predicted. This observation is consistent with the observation that the maximum in the observed momentum density is at lower momentum than is predicted. The result reflects the left-right electron correlation, which causes electron density to pile up at opposite ends of the molecule at the expense of electron density in the middle.

### Conclusion

The usefulness of the (e,2e) technique for atomic and molecular systems was first suggested by physicists<sup>20</sup> with training in nuclear physics where (p,2p) and ( $\alpha,2\alpha$ ) experiments have been used to investigate nucleon momentum densities. There are, in addition to our group, three other groups (Flinders University, in Australia,<sup>21</sup> C.N.E.N. in Frascati, Italy,<sup>22</sup> and the

(20) Baker, G. A.; McCarthy, I. E.; Porter, C. E. *Phys. Rev.* 1960, 120, 254. Smirnov, Yu. F.; Neudatchin, V. G. *JETP Lett. (Engl. Transl.)* 1966, 3, 192. Glassgold, A. E. "Abstracts of Papers, ICPEAC V" 1967, 646.

(21) Weigold, E.; Hood, S. T.; McCarthy, I. E.; Tuebner, P. J. O. *Phys. Lett. A*, 1973 44, 531. Hood, S. T.; Weigold, E.; McCarthy, I. E.; Tuebner, P. J. O. *Phys. Sci.* 1973, 245, 65. Hood, S. T.; McCarthy, I. E.; Tuebner, P. J. O.; Weigold, E. *Phys. Rev. A* 1974, 9, 260. Weigold, E.; Hood, S. T.; McCarthy, I. E. *Ibid.* 1975, 11, 566. Dey, S.; McCarthy, I. E.; Tuebner, P. J. O.; Weigold, E. *Phys. Rev. Lett.* 1975, 34, 782. Dey, S.; Dixon, A. J.; Lassey, K. R.; McCarthy, I. E.; Tuebner, P. J. O.; Weigold, E.; Bagus, P. S.; Viinikka, E. K. *Phys. Rev. A* 1977, 15, 102. Dey, S.; Dixon, A. J.; McCarthy, I. E.; Weigold, E. *J. Electron Spectrosc. Relat. Phenom.* 1976, 9, 397. Weigold, E.; Dey, S.; Dixon, A. J.; McCarthy, I. E.; Lassey, K. R.; Tuebner, P. J. O. 1977, 10, 177. Dixon, A. J.; Dey, S.; McCarthy, I. E.; Weigold, E.; Williams, G. R. *J. Chem. Phys.* 1977, 21, 81. Dixon, A. J.; McCarthy, I. E.; Weigold, E.; Williams, G. R. *J. Electron Spectrosc. Relat. Phenom.* 1977, 12, 239. Dixon, A. J.; Hood, S. T.; Weigold, E.; Williams, G. R. *J. Ibid* 1978, 14, 267. Weigold, E.; Noble, C. Hood, S. T.; Fuss, I. *ibid* 1979, 15, 253. Brion, C. E.; McCarthy, I. E.; Suzuki, I. H.; Weigold, E. *Chem. Phys. Lett.* 1979, 67, 115. Suzuki, I. H.; Weigold, E.; Brion, C. E. *J. Electron Spectrosc. Relat. Phenom.* 1980, 20, 289. Brion, C. E.; Hood, S. T.; Suzuki, I. H.; Weigold, E.; Williams, G. R. *J. Ibid* 1980, 21, 71.

University of British Columbia in Canada).<sup>23</sup> Together more than 50 atoms and molecules have been studied from He and H<sub>2</sub> to Xe and C<sub>6</sub>H<sub>6</sub>. It is noteworthy that in cases where more than one group has studied a system, the experimental agreement has always been well within the reported experimental errors. Though many systems have been investigated, there seems to be a large number of interesting systems yet to be studied. Also, as experimental techniques improve and more precise measurements can be made, much of the ground which has already been covered can be profitably revisited.

A number of elements of the experimental apparatus must be improved in order to improve the flexibility of the technique and to increase the quality of the data. Confidence in the simple approximations employed to analyze the data would be increased if the incident electron energies were raised from the present 400–1200 eV to 1500–5000 eV. An increase in incident energy

would also allow one to probe the inner electrons of molecules where correlation effects are important. The state-of-the-art energy resolution is now approximately 1 eV. In many molecules the ionization energies are so closely spaced that an improvement in energy resolution of about a factor of 5 would be of great value. With present instruments, several days may be required to obtain a single momentum distribution. Both the flexibility of the experiment and the precision of the data will be improved as multiplexed instruments such as ours become more highly developed. The angular resolution and hence the momentum resolution of present instruments appear to be adequate for chemical studies; however, the desired improvements mentioned above are not easily obtained without degrading angular resolution. It follows that future designs will be preceded by careful study of the electron optics and the electronics of the (e,2e) apparatus.

As is evident from our discussion above, much of our (e,2e) work has focused upon  $\pi$  bonding in hydrocarbons. In the near future, other applications of the experiment are already apparent. One is the study of bonding to heavy atoms with emphasis upon organometallic complexes. Another is the study of electron correlation through the observation of momentum densities associated with satellite structure. Yet another area is the investigation of the properties of the unpaired and nonbonding pairs of electrons where it is expected that the  $\Delta B(r)$  analysis will play an important role in the interpretation of the data.

The momentum space view of chemistry afforded by (e,2e) spectroscopy has contributed new insight into chemical bonding and the single electron description of electronic behavior, while the use of the  $B(r)$  function has helped in the interpretation of the experimental results. As new and better data become available, it is not unreasonable to expect the (e,2e) technique to rival photoelectron spectroscopy as the method of choice for the investigation of electronic structure in molecules.

*This work has been supported by the National Science Foundation and by the Computer Science Center of the University of Maryland.*

(22) Botticelli, Antonio; Camilloni, Rossana; Giardini Guidoni, Anna; Missoni, Guido; Stefani, Giovanni; Tiribelli, Roberto; Vinciguerra, Damiano *Ann. Chim. (Rome)* **1974**, *64*, 189. Camilloni, R.; Stefani, G.; Giardini-Guidoni, A.; Tiribelli, R.; Vinciguerra, D. *Chem. Phys. Lett.* **1976**, *41*, 17. Giardini-Guidoni, A.; Tiribelli, R.; Vinciguerra, D.; Camilloni, R.; Stefani, G. *J. Electron Spectrosc. Relat. Phenom.* **1977**, *12*, 405. Giardini-Guidoni, A.; Fantoni, R.; Tiribelli, R.; Vinciguerra, D.; Camilloni, R.; Stefani, G. *J. Chem. Phys.* **1979**, *71*, 3182. Giardini-Guidoni, A.; Fantoni, R.; Tiribelli, R.; Marconero, R.; Camilloni, R.; Stefani, G. *Phys. Lett. A* **1980**, *77a*, 19. Fantoni, R.; Giardini-Guidoni, A.; Tiribelli, R.; Camilloni, R.; Stefani, G. *Chem. Phys. Lett.* **1980**, *71*, 335. Giardini-Guidoni, Anna; Camilloni, Rossana; Stefani, Giovanni *Ann. Chim. (Rome)* **1977**, *67*, 631. Giardini-Guidoni, A.; Fantoni, R.; Camilloni, R.; Stefani, G. *Comments At. Mol. Phys.* **1981**, *10*, 107. Cambi, R.; Ciullo, G.; Sgamellotti, A.; Tarantelli, F.; Fantoni, R.; Giardini-Guidoni, A.; Sergio, A. *Chem. Phys. Lett.* **1981**, *80*, 295.

(23) Hood, S. T.; Hamnett, A.; Brion, C. E. *Chem. Phys. Lett.* **1976**, *29*, 252. Brion, C. E.; Cook, J. P. D.; Tan, K. H. *Ibid.* **1978**, *59*, 241. Cook, J. P. D.; Brion, C. E.; Hamnett, A. *J. Electron Spectrosc. Relat. Phenom.* **1979**, *15*, 233. Hood, S. T.; Hamnett, A.; Brion, C. E. *Chem. Phys. Lett.* **1976**, *41*, 428. Hood, S. T.; Hamnett, A.; Brion, C. E. *J. Electron Spectrosc. Relat. Phenom.* **1977**, *11*, 205. Hamnett, A.; Hood, S. T.; Brion, C. E. *J. Electron Spectrosc. Relat. Phenom.* **1977**, *11*, 263. Brion, C. E.; McCarthy, I. E.; Suzuki, I. H.; Weigold, E. *Chem. Phys. Lett.* **1979**, *67*, 115. Cook, J. P. D.; Brion, C. E.; Hamnett, A. *Chem. Phys.* **1980**, *45*, 1. Suzuki, I. H.; Brion, C. E.; Weigold, E.; Williams, G. R. *J. Int. J. Quantum Chem.* **1980**, *18*, 275. Suzuki, I. H.; Weigold, E.; Brion, C. E. *J. Electron Spectrosc. Relat. Phenom.* **1980**, *20*, 289. Brion, C. E.; Hood, S. T.; Suzuki, I. H.; Weigold, E.; Williams, G. R. *J. ibid.* **1980**, *21*, 71.